Eur. Phys. J. D **42**, 373–379 (2007)
DOI: 10.1140/epjd/e2007-00048-2

THE EUROPEAN PHYSICAL JOURNAL D

Spontaneously generated coherence in a Doppler broadened atomic system

A.-J. Li[1,2,a], C.-L. Wang[1,2], L. Wang[1,2], J.-H. Wu[1,2], and J.-Y. Gao[1,2]

[1] Key Laboratory of Coherent Light, Atomic and Molecular Spectroscopy, Ministry of Education (Jilin University), Changchun 130023, P.R. China
[2] College of Physics, Jilin University, Changchun 130023, P.R. China

Received 14 November 2006 / Received in final form 25 December 2006
Published online 7 March 2007 –

Abstract. We investigate the spontaneously generated coherence (SGC) in a Doppler broadened four-level atomic system driven by two coherent fields. We plot the spontaneous emission spectra with different parameters and discuss how the initial atomic conditions and parameters of both fields change the number of peaks and dark lines of spontaneous emission spectra. Furthermore, we also show how the spontaneous emission spectrum is modified by Doppler effects in the viewed direction. Our results have important references to the experimental observation of SGC in hot atomic vapors.

PACS. 32.80.Qk Coherent control of atomic interactions with photons – 32.50.+d Fluorescence, phosphorescence (including quenching) – 42.50.Lc Quantum fluctuations, quantum noise, and quantum jumps

1 Introduction

Spontaneous emission coherence has attracted much attention for many years, which is also referred as spontaneously generated coherence (SGC). Spontaneous emission is probably one of the best known fundamental processes based on the interaction between radiation and matter. Phenomena resulting from SGC are closely related with lasing without inversion [1], transparent high-index materials [2], high-precision spectroscopy and magnetometer [3], quantum information and computing [4], etc. A lot of theoretical works have been devoted to discuss these effects, it has been predicted that SGC can lead to many interesting results, such as a dark line in spontaneous emission spectrum, the narrowing down, suppression or complete cancellation of spontaneous emission, the enhancement of spontaneous emission, and phase sensitive spontaneous emission and absorption spectra [5,6]. However, it is very difficult to demonstrate them experimentally for the rigorous conditions of near degenerate close-lying levels and non-orthogonal dipole matrix elements. A feasible scheme is proposed to observe the SGC in a four-level atomic system [7], where the spontaneous emission spectra show the interesting SGC phenomena such as the narrow enhanced peak and fluorescence quenching point. In this paper, we study further the spontaneous emission spectra with different initial atomic conditions and show the fluorescence total quenching with appropriate parameters. Next the effects of initial atomic conditions and parameters of both fields on the spontaneous emission spectra are discussed. Moreover, we also show how the spontaneous emission spectrum is modified by Doppler effects in the viewed direction. Spontaneous emission spectra with and without Doppler shifts is compared to show the Doppler effects. It is proved that the Doppler widths play an important role in the experiments of observation of SGC in hot atomic vapors.

[a] e-mail: liaijun0405@126.com

2 Calculation and analysis

The four-level Rb atomic system is depicted in Figure 1a. One coherent pumping field with frequency ω_p and amplitude E_p is used to drive the D_2 line $5S_{1/2}(F=1) \leftrightarrow 5P_{3/2}$ transitions. Another coherent coupling field with frequency ω_c and amplitude E_c is used to drive $5P_{3/2} \leftrightarrow 5D_{5/2}$ transitions. Atoms in level $5P_{3/2}$ spontaneously decay to level $5S_{1/2}(F=2)$ with rate Γ_2. $\Delta_p = \omega_{21} - \omega_p$ and $\Delta_c = \omega_{32} - \omega_c$ are detunings of the pumping and coupling field, respectively.

With the rotating-wave and electric-dipole approximations, and the assumption of Planck constant $\hbar = 1$, the interaction Hamiltonian for the system under study can be written as

$$H_I = \sum_k \{g_{k,24} \exp(i\delta_k t)\, b_k |2\rangle\langle 4|\} + \Omega_p \exp(i\Delta_p t)\, |2\rangle\langle 1| + \Omega_c \exp(i\Delta_c t)\, |3\rangle\langle 2| + H.c. \quad (1)$$

$$S(\delta_k) = \frac{\Gamma_2}{2\pi}\left|\frac{a_2(0)(\delta_k-\Delta_p)(\delta_k+\Delta_c) - i\Omega_p a_1(0)(\delta_k+\Delta_c) - i\Omega_c a_3(0)(\delta_k-\Delta_p)}{(-\delta_k+i\frac{\Gamma_2}{2})(\delta_k-\Delta_p)(\delta_k+\Delta_c)+\Omega_p^2(\delta_k+\Delta_c)+\Omega_c^2(\delta_k-\Delta_p)}\right|^2 \tag{5}$$

$$S(\delta_k) = \int_{-\infty}^{+\infty}\int_{-\infty}^{+\infty}\frac{\Gamma_2}{2\pi}\left|\frac{a_2(0)(\delta_k'-\Delta_p')(\delta_k'+\Delta_c') - i\Omega_p a_1(0)(\delta_k'+\Delta_c') - i\Omega_c a_3(0)(\delta_k'-\Delta_p')}{(-\delta_k'+i\frac{\Gamma_2}{2})(\delta_k'-\Delta_p')(\delta_k'+\Delta_c')+\Omega_p^2(\delta_k'+\Delta_c')+\Omega_c^2(\delta_k'-\Delta_p')}\right|^2 N(\upsilon_x,\upsilon_y)d\upsilon_x d\upsilon_y \tag{6}$$

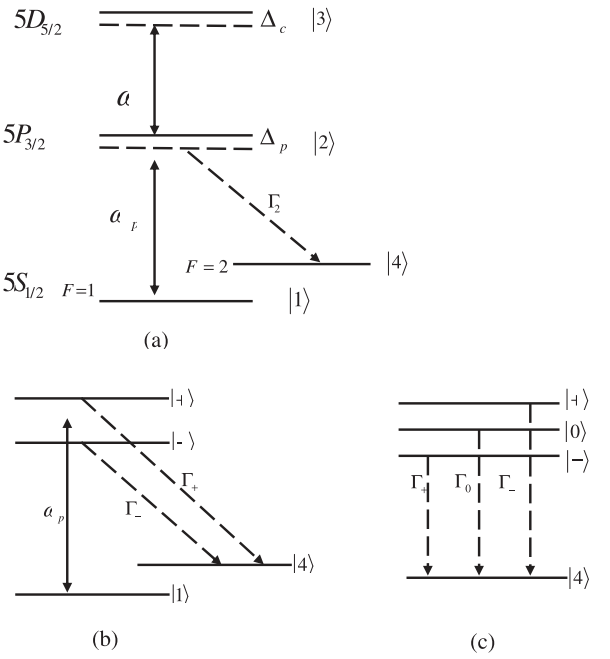

Fig. 1. (a) Schematic representation of the relevant Rb atomic energy levels; (b) the atomic energy levels in the partially dressed state picture; (c) the atomic energy levels in the fully dressed state picture.

where b_k^+ and b_k are the creation and annihilation operators for the kth vacuum mode with frequency ω_k, respectively; $\delta_k = \omega_{24} - \omega_k$ is the detuning of the kth vacuum mode, $g_{k,24}$ is the coupling constant between the kth vacuum mode and the transition between $|2\rangle$ and $|4\rangle$; Ω_p and Ω_c are Rabi frequencies of the pumping and coupling fields, respectively.

The state vector at time t can be written as

$$|\Psi_I(t)\rangle = [a_1(t)|1\rangle + a_2(t)|2\rangle + a_3(t)|3\rangle]|\{0\}\rangle + \sum_k a_{4,k}(t)|4\rangle|1_k\rangle \tag{2}$$

where $|\{0\}\rangle$ denotes the vacuum mode of the radiation field. The evolution of the state vector obeys the well-known Schrödinger equation

$$\frac{d}{dt}|\Psi_I(t)\rangle = -\frac{i}{\hbar}H_I(t)|\Psi_I(t)\rangle. \tag{3}$$

Substituting equation (1) and equation (2) into equation (3), and using the Weisskopf-Wigner theory [8–10], we obtain the following equations for the probability amplitudes

$$\dot{a}_1(t) = -i\Omega_p \exp(-i\Delta_p t)a_2(t) \tag{4a}$$

$$\dot{a}_2(t) = -i\Omega_p \exp(i\Delta_p t)a_1(t) - \frac{\Gamma_2}{2}a_2(t) - i\Omega_c \exp(-i\Delta_c t)a_3(t) \tag{4b}$$

$$\dot{a}_3(t) = -i\Omega_c \exp(i\Delta_c t)a_2(t) \tag{4c}$$

$$\dot{a}_{4,k}(t) = -ig_{k,24}\exp(-i\delta_k t)a_2(t). \tag{4d}$$

Here $\Gamma_2 = 2|\vec{\mu}_{24}|^2\omega_{24}^3/3\pi\varepsilon_0\hbar c^3$ is the population decay rate of level $|2\rangle$, and $\vec{\mu}_{24}$ is the matrix element of the dipole moment of the transition between level $|2\rangle$ and level $|4\rangle$.

The spontaneous emission spectrum is the Fourier transform of $\langle E^-(t+\tau)E^+(t)\rangle_{t\to\infty}$, and can be written as $S(\delta_k) = \Gamma_0|a_{4,k}(t\to\infty)|^2 \big/ 2\pi|g_{k,24}|^2$ for the emission from level $|2\rangle$ to level $|4\rangle$ [11]. We use the Laplace transform method [12] and the final value theorem to obtain the spontaneous emission spectrum as following

see equation (5) above

where $a_1(0), a_2(0), a_3(0), a_4(0)$ are number of the initial atoms populated in levels $|1\rangle$, $|2\rangle$, $|3\rangle$, $|4\rangle$, respectively.

In a Doppler broadened system, the detunings of both fields can be written as $\Delta_p' = \Delta_p + k_p\upsilon_y$, $\Delta_c' = \Delta_c + k_c\upsilon_y$, $\delta_k' = \delta_k + \kappa_p(\upsilon_x\sin(\theta) + \upsilon_y\cos(\theta))$, respectively. If the coherent driving field and pumping field propagate along the y-axis, and the fluorescence is collected in the direction having an angle θ with the y-axis on the x-y plane, then the spontaneous emission spectrum can be described by

see equation (6) above

where $N(\upsilon_x,\upsilon_y) = (N_0/2\pi u^2)e^{-\left(\upsilon_x^2+\upsilon_y^2\right)/2u^2}$ (u is the room-mean-square atomic velocity and N_0 is the total atomic number density) is the Maxwellian velocity distribution on the x-y plane in a Doppler-broadened system, and the Gaussian line width is $D = 2\sqrt{\ln 2}ku$. We set $N_0 = 500\times10^{12}$, $\lambda_p = 780$ nm, $\lambda_c = 776$ nm, $\Gamma_2 = 3$ MHz and $u = 237$ m/s for room-temperature in the calculation.

In order to show further the SGC effect in this atomic system, we derive the equations in the partially dressed state picture of the coupling field ω_c, where levels $|2\rangle$ and $|3\rangle$ can be replaced by two levels $|+\rangle$ and $|-\rangle$ (see Fig. 1b), whose probability amplitudes are given by

$$a_+ = (\cos\theta)a_2 + (\sin\theta)a_3 \tag{7a}$$

$$a_- = (\sin\theta)a_2 - (\cos\theta)a_3 \tag{7b}$$

with $\tan\theta = \omega_+/\Omega_c$ and $\omega_\pm = (\Delta_c \pm \sqrt{\Delta_c^2 + 4\Omega_c^2})/2$ being eigenfrequencies of levels $|+\rangle$ and $|-\rangle$. With equations (7), we can replace equations (4) by

$$\dot{a}_1(t) = -i(\Omega_{+1}a_+ + \Omega_{-1}a_-) \tag{8a}$$

$$\dot{a}_+(t) = -i\Omega_{+1}a_1 - (\Gamma_+/2 + i\Delta_+)a_+ - (\Gamma_{+-}/2)a_- \tag{8b}$$

$$\dot{a}_-(t) = -i\Omega_{-1}a_1 - (\Gamma_-/2 + i\Delta_-)]a_- - (\Gamma_{+-}/2)a_+ \tag{8c}$$

$$\dot{a}_{4,k}(t) = -i(\Delta - \delta_k)a_{4,k} - i(g_{k+}a_+ + g_{k-}a_-) \tag{8d}$$

where $\Delta_+ = \Delta_p + \Omega_c \sin 2\theta + \Delta_c \sin^2\theta$, $\Delta_- = \Delta_p - \Omega_c \sin 2\theta + \Delta_c \cos^2\theta$, $\Gamma_+ = \Gamma_2 \cos^2\theta$, $\Gamma_- = \Gamma_2 \sin^2\theta$, $\Gamma_{+-} = (\Gamma_2/2 - i\Delta_c)\sin 2\theta - 2i\Omega_c \cos 2\theta$, $\Omega_{+1} = \Omega_p \cos\theta$, $\Omega_{-1} = \Omega_p \sin\theta$, $g_{k+} = g_{k,24}\cos\theta$, $g_{k-} = g_{k,24}\sin\theta$. From equations (8b) and (8c), we can see that there exists quantum interference between the two spontaneous emission channels $|+\rangle \to |4\rangle$ and $|-\rangle \to |4\rangle$ because $a_+(t)$ and $a_-(t)$ are driven mutually by Γ_{+-}.

In order to have a non-vanishing steady-state population in levels $|1\rangle$, $|+\rangle$, and $|-\rangle$, we find from equations (8) that the following equation should be fulfilled:

$$\Omega_{+1}^2(\Gamma_-/2 + i\Delta_-) + \Omega_{-1}^2(\Gamma_+/2 + i\Delta_+) = \Omega_{+1}\Omega_{-1}\Gamma_{+-}. \tag{9}$$

The real part of equation (9) is always zero, while the vanishing of its imaginary part requires $\Delta_p + \Delta_c = 0$. That is, when $\Delta_p + \Delta_c \neq 0$, all atoms will decay to level $|4\rangle$, and we have the general result of $a_1(\infty) = a_-(\infty) = a_+(\infty) = 0$. Conversely, some atoms will be trapped in levels $|1\rangle$, $|+\rangle$, and $|-\rangle$ if $\Delta_p + \Delta_c = 0$. As usual, here we call $\Delta_p + \Delta_c = 0$ as coherent population trapping (CPT) condition [13]. We plot the time evolutions of ρ_{11}, ρ_{++}, and ρ_{--} for different parameters that satisfy the CPT condition or not. From Figure 2a, we can see that when $\Delta_p + \Delta_c = 0$, there are non-vanishing population distributions for a long time in levels $|1\rangle$, $|+\rangle$ and $|-\rangle$, which means that some atoms are trapped in these levels. When $\Delta_p + \Delta_c \neq 0$, however, population distributions in levels $|1\rangle$, $|+\rangle$ and $|-\rangle$ are constantly zero for a long time as shown in Figure 2b.

During the preceding calculation, we neglect the following decays: $|3\rangle \to |2\rangle$, $|2\rangle \to |1\rangle$ and $|1\rangle \to |4\rangle$, which will bring a small deviation to the decays in the partially dressed state picture. According to the conclusion in [14], the decays above have little effect on the result: the decays along the drive transitions $|+\rangle \to |1\rangle$, $|-\rangle \to |1\rangle$ and $|1\rangle \to |4\rangle$ (due to collisions, for example) can make the SGC effect more pronounced, and the additional decays along the transition $|+\rangle \to |-\rangle$ add population to the nondecaying state and consequently more population are trapped in the upper levels. There is no fundamental change on the SGC phenomena if considering these decays. So we neglect them during the calculation, since we can expect a clearer analytic solution in this way.

3 Numerical results and discussion

In this section, we show a few spontaneous emission spectra based on the numerical calculation above. Figures 3a–6a show spontaneous emission spectra with different initial atomic conditions and parameters of both fields and Figures 3b–6b show corresponding spontaneous emission spectra with Doppler effects. Figure 7 shows the difference of the spectra between the co-propagating case and the counter-propagating case. The viewed angle is $\theta = \pi/4$ in Figures 3–7 and Figure 8 shows the effects of the viewed angle on the spontaneous emission spectra.

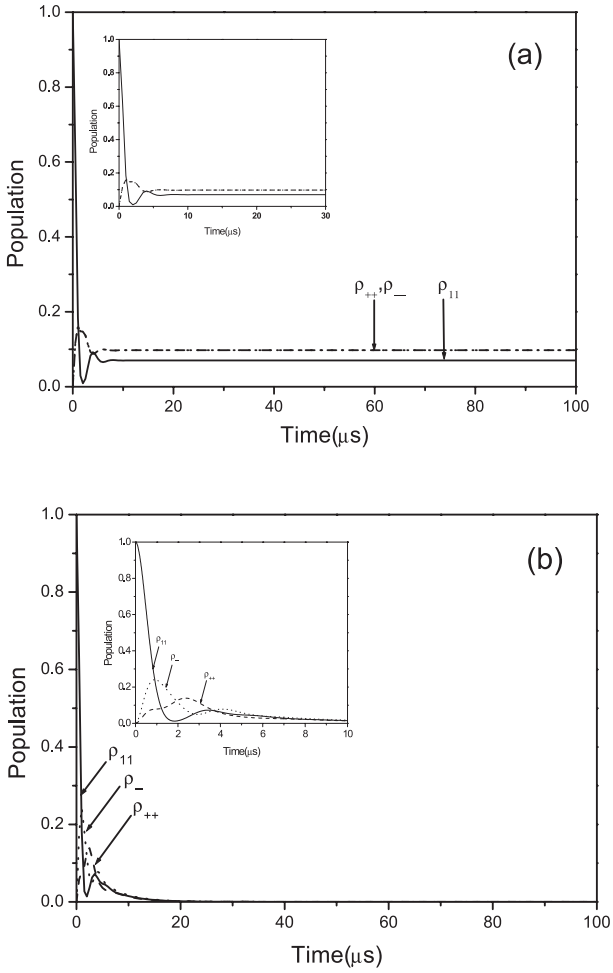

Fig. 2. Time evolution of atomic populations in the partially dressed levels $|1\rangle$, $|+\rangle$ and $|-\rangle$ for $\Omega_p = 1.5$ MHz, $\Omega_c = 0.9$ MHz, $\Delta_p = 0.0$ MHz. (a) $\Delta_c = 0.0$ MHz; (b) $\Delta_c = 1.0$ MHz.

In the fully dressed states picture, levels $|1\rangle$, $|2\rangle$, $|3\rangle$ and both fields ω_p and ω_c can be replaced by three new states $|+\rangle$, $|0\rangle$ and $|-\rangle$ as shown in Figure 1c. So there will be three peaks corresponding to the spontaneous emission from three dressed states to the level $|4\rangle$ as shown in Figures 3a and 4a. Before atoms spontaneously decay to the final level, they could go through three different pathways $|-\rangle \to |4\rangle$, $|0\rangle \to |4\rangle$ and $|+\rangle \to |4\rangle$ when they are pumped into the intermediate level. Different transition pathways interfere each other and result in the narrow peak or dark line in the spontaneous emission spectra. These features are different from the uncoherent spectra, which are the simple uncoherent overlap of several Gaussian shapelines.

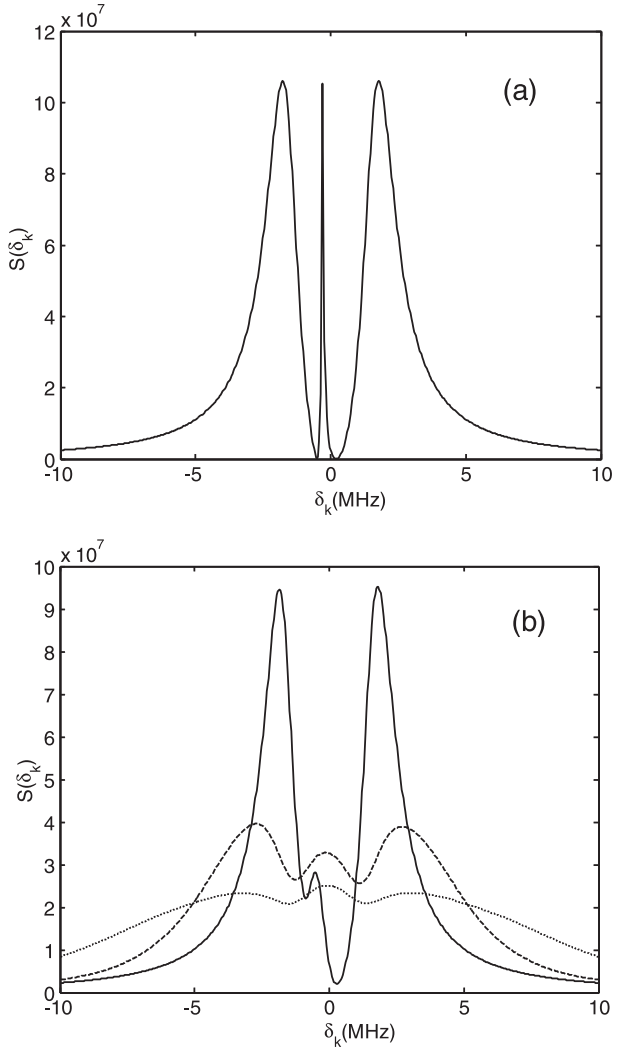

Fig. 3. Spontaneous emission spectra $S(\delta_k)$ with two dark lines for $\Delta_c = 0.5$ MHz, $\Delta_p = 0.2$ MHz, $\Omega_p = 1.5$ MHz, $\Omega_c = 0.9$ MHz, and $a_1(0) = a_3(0) = 0$, $a_2(0) = 1$. (a) Spectra for free of Doppler shifts; (b) spectra with Doppler widths D of 0.507 MHz (solid), 5.07 MHz (dashed) and 10.14 MHz (dotted).

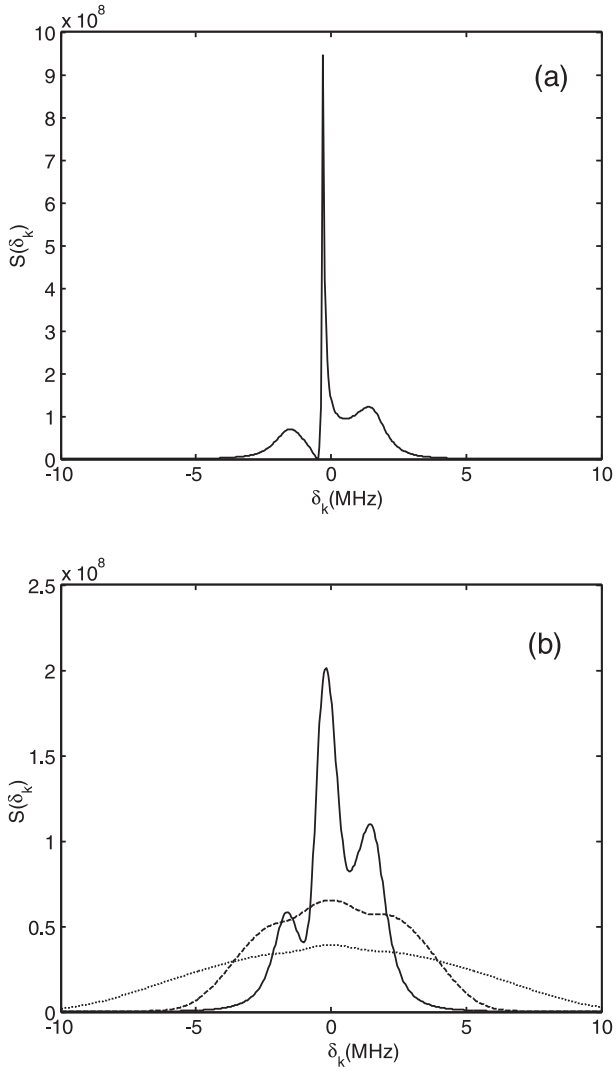

Fig. 4. Spontaneous emission spectra $S(\delta_k)$ with one dark line for $\Delta_c = 0.5$ MHz, $\Delta_p = 0.2$ MHz, $\Omega_p = 1.5$ MHz, $\Omega_c = 0.9$ MHz, and $a_1(0) = 1$, $a_2(0) = a_3(0) = 0$. (a) Spectra for free of Doppler shifts; (b) spectra with Doppler widths D of 0.507 MHz (solid), 5.07 MHz (dashed) and 10.14 MHz (dotted).

When the CPT condition $\Delta_p + \Delta_c = 0$ is fulfilled, part of the population is confined to the dark state. In this case, two peaks are expected because the central peak has no contribution from level $|2\rangle$ (transitions from level $|1\rangle$ and level $|3\rangle$ to level $|4\rangle$ are forbidden), which is supported by the double peaks spectrum in Figure 5a. Under the CPT condition, choosing initial atomic conditions properly, all the atoms are populated in the dark state due to the strongly spontaneous emission interference. In this case, the total fluorescence quenching can be found as shown in Figure 6a.

The number of peaks of spontaneous emission spectra can be controlled by CPT conditions as discussed above. In the case of three peaks, the number of dark lines can be controlled by initial atomic conditions. Two dark lines appear in spontaneous emission spectra only when the initial atomic condition $a_2(0) \neq 0$, i.e., some atoms must be populated in level $|2\rangle$ as shown in Figure 3a. When initial atoms totally populated in level $|1\rangle$ or level $|3\rangle$, the spontaneous emission coherence can give rise to one dark line in the spectra as shown in Figure 4a.

We show the effects of Doppler shifts on the spontaneous emission spectra in all the cases discussed above in Figures 3b–6b. Comparing the spectra with and without Doppler shifts, we find that the SGC phenomena in this hot atomic system are sensitive to Doppler effects. Large Doppler shifts will result in weaken quantum interference among the following transition pathways: $|-\rangle \rightarrow |4\rangle$, $|0\rangle \rightarrow |4\rangle$ and $|+\rangle \rightarrow |4\rangle$, then the distinct SGC features, such as narrow peaks and dark lines, will be blurred with large Doppler widths. In the case of two dark lines in spontaneous emission spectra as shown in Figure 3b, we can see that the narrow central peak reduces rapidly and both side peaks also become wider and shorter with increasing

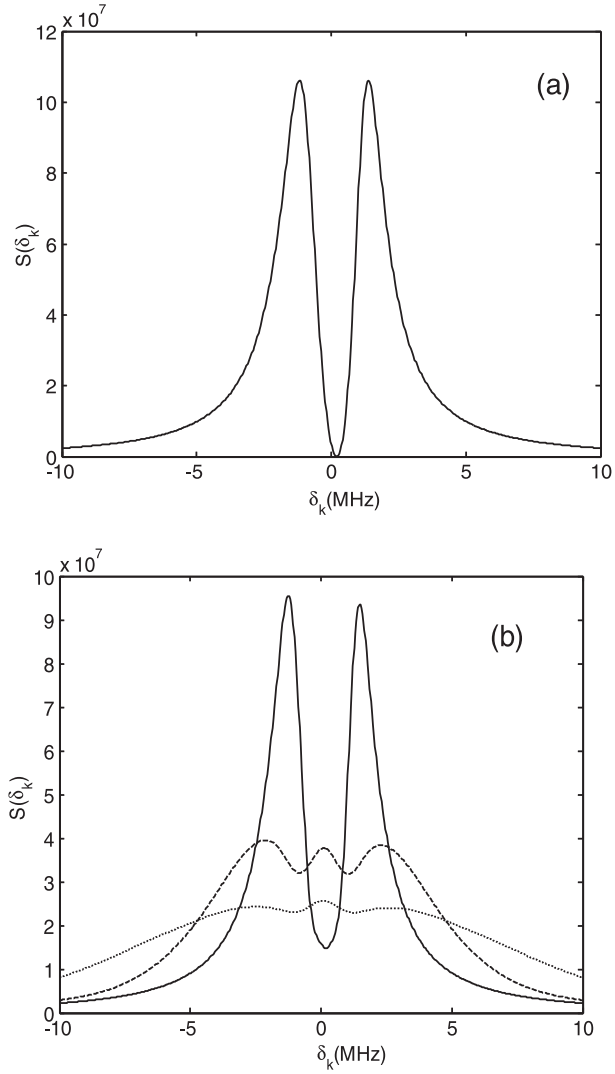

Fig. 5. Spontaneous emission spectra $S(\delta_k)$in CPT conditions for $a_1(0) = a_3(0) = 0$, $a_2(0) = 1$, $\Delta_c = -0.2$ MHz, $\Delta_p = 0.2$ MHz, $\Omega_p = \Omega_c = 0.9$ MHz. (a) Spectra for free of Doppler shifts; (b) spectra with Doppler widths D of 0.507 MHz (solid), 5.07 MHz (dashed) and 10.14 MHz (dotted).

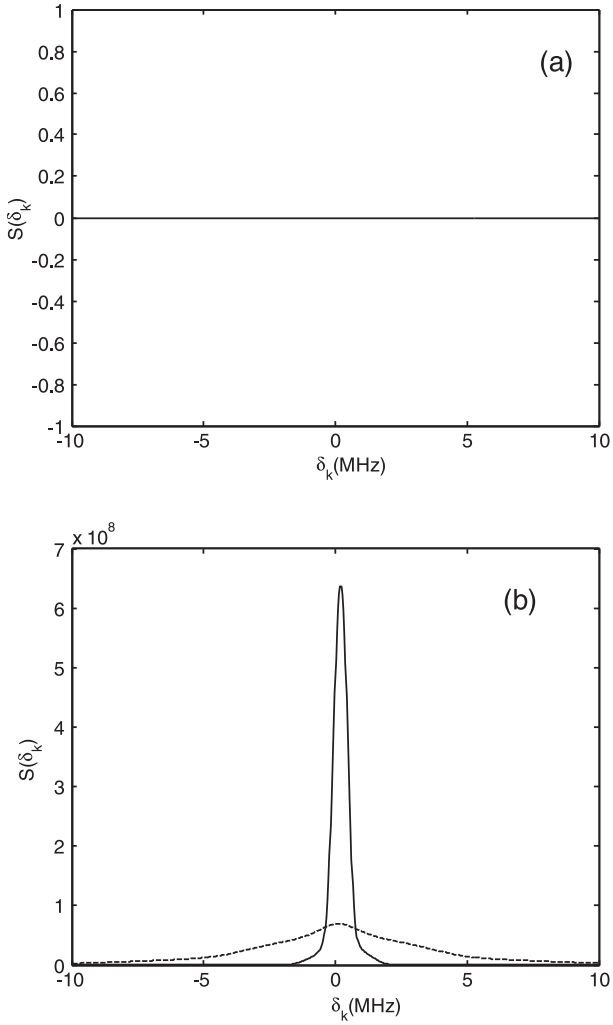

Fig. 6. Doppler effects on fluorescence quenching of the spectra $S(\delta_k)$ for $a_1(0) = 0.707$, $a_2(0) = 0$, $a_3(0) = -0.707$, $\Delta_c = -0.2$ MHz, $\Delta_p = 0.2$ MHz, $\Omega_p = \Omega_c = 0.9$ MHz. (a) The spontaneous emission spectra for free Doppler broadening; (b) spectra with Doppler widths D of 0.507 MHz (solid), and 5.07 MHz (dashed).

Doppler widths. The narrow central peak and two dark lines result from SGC disappear and are replaced by one peak when the Doppler width increased to 10.14 MHz. In one dark line case as shown in Figure 4b, the dark line weaken and the narrow central peak becomes wider and lower with increasing Doppler widths, which are more sensitive than two dark lines. And the spontaneous emission spectrum becomes a low Gaussian shape peak when the Doppler widths increase to 10.14 MHz. In Figure 5b, we can see that a small central peak appears between the two peaks with increasing Doppler shifts, the reason is that the increasing Doppler shifts make the parameters not satisfy the CPT condition anymore. The CPT condition is destroyed by the increasing Doppler widths and the spontaneous emission spectra show the same features as that in Figure 3b with initial atoms populated in level $|2\rangle$. In Figure 6a, we can see the fluorescence total quenching in the spontaneous emission spectra for free of Doppler effects. The fluorescence quenching disappears and is replaced by a peak as soon as there is any Doppler width as shown in Figure 6b. All the discussion above is based on the co-propagation of both coherent and pump fields, the SGC features in spontaneous emission spectra are more sensitive to the Doppler widths in the case of counter-propagation of both fields, which are shown in Figure 7. Under the same conditions, the central narrow peak in co-propagation of both fields even disappears in the case of counter-propagation as shown in Figure 7a.

At last, we show the spontaneous emission spectra with Doppler width 0.507 MHz in different viewed angles in Figure 8, from which we can see that the height of the central peak becomes higher with increasing viewed angle from 0 to π in general.

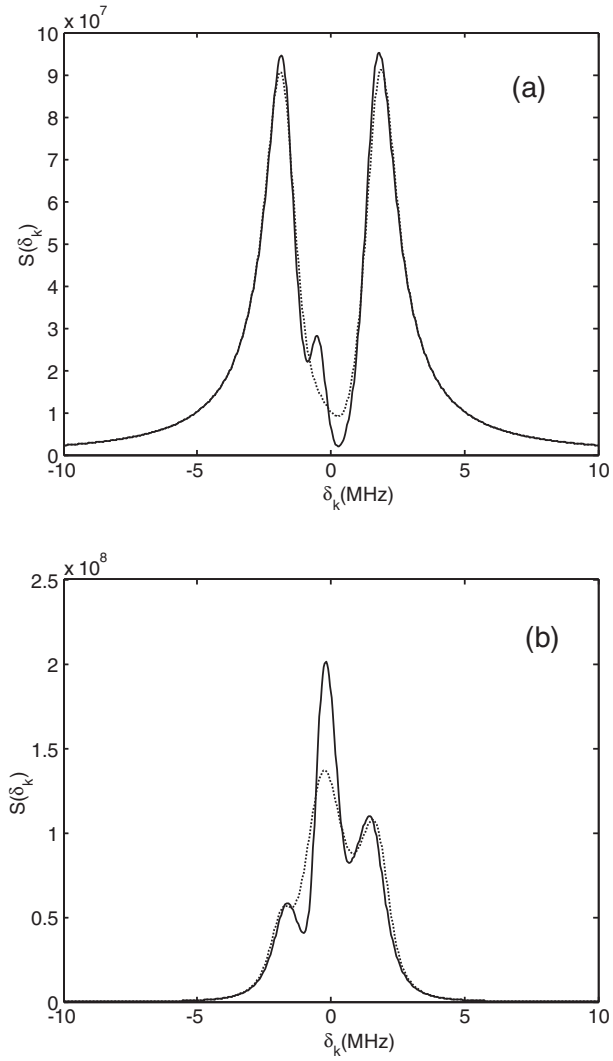

Fig. 7. Doppler effects on spontaneous emission spectra $S(\delta_k)$ for co-propagation (solid) and counter-propagation (dotted) of both fields with Doppler width 0.507 MHz, $\Delta_c = 0.5$ MHz, $\Delta_p = 0.2$ MHz, $\Omega_p = 1.5$ MHz, $\Omega_c = 0.9$ MHz. (a) $a_1(0) = a_3(0) = 0$, $a_2(0) = 1$; (b) $a_1(0) = 1$, $a_2(0) = a_3(0) = 0$.

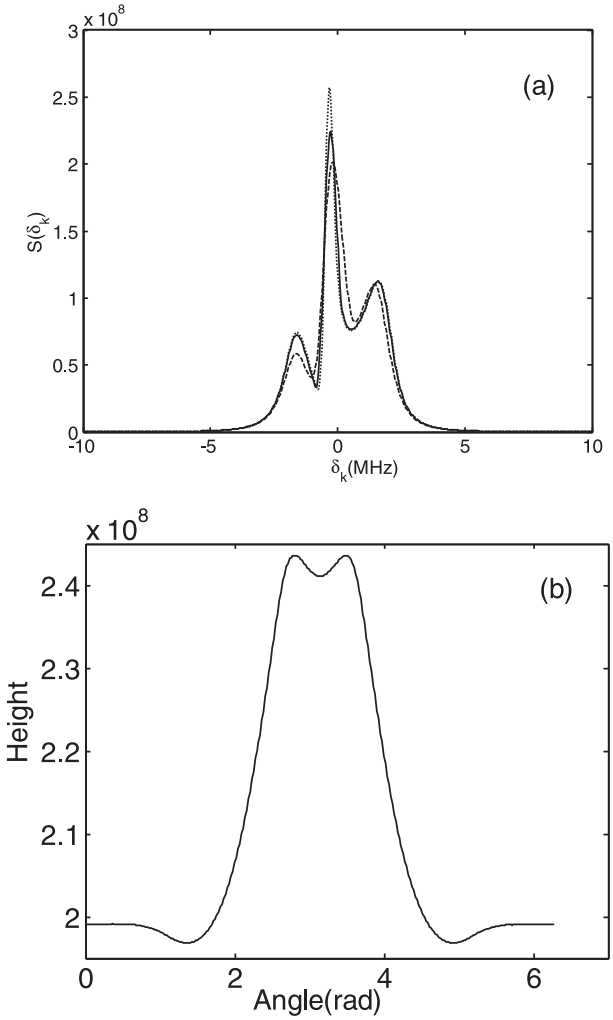

Fig. 8. Spontaneous emission spectra $S(\delta_k)$ with Doppler width 0.507 MHz in different viewed angle for$\Delta_c = 0.5$ MHz, $\Delta_p = 0.2$ MHz, $\Omega_p = 1.5$ MHz, $\Omega_c = 0.9$ MHz and $a_1(0) = 1$, $a_2(0) = a_3(0) = 0$. (a) The dashed line stands for $\theta = \pi/4$, the solid line stands for $\theta = 3\pi/4$, and dotted line stands for $\theta = 7\pi/8$; (b) the height of the central peak at $\delta_k = -0.25$ MHz with different viewed angles.

4 Conclusions

In this paper, we investigate SGC phenomena of the spontaneous emission spectra in a Doppler broadened four-level atomic system. Different spectra lineshapes are plot with different initial atomic conditions and CPT conditions. We find that CPT conditions determine the peaks number of the spontaneous emission spectra and initial atomic conditions determine the dark lines number of the spontaneous emission spectra. Further more, a completed survey of Doppler effects on the spontaneous emission spectra is given with different parameters. In the case of three peaks, the distinct SGC features such as dark line and narrow peak are destroyed gradually by increasing Doppler widths. In CPT conditions, including the case of double peaks and totally fluorescence quenching, the spontaneous emission spectra are more sensitive to the Doppler widths, and the totally fluorescence quenching disappear even with small Doppler widths. The spontaneous emission spectra are more significantly modified by the Doppler widths in the counter-propagation of both coherent and pump fields than that in the co-propagation case. Comparing the spontaneous emission spectra with and without Doppler shifts, we find that the spontaneous emission spectra are sensitive to the Doppler broadening, and some of the relevant SGC features are preserved only when the Doppler width is small. Since experiments in nonlinear optics and spectroscopy are often performed in atomic vapors, where the linewidths of the transitions are dominated by Doppler broadening, and few work is devoted to discussing Doppler effects on the spontaneous emission spectra before. Our results provide valuable reference for carrying the experiments for observation of SGC in atomic vapors.

The authors would like to thank the support from the National Natural Science Foundation of China under the Grant Number of 10334010, support from the doctoral program foundation of institution of High Education of China, and from the special foundation program, "Quantum Control", by the NMST.

References

1. S.E. Harris, Phys. Rev. Lett. **62**, 1033 (1989); J.Y. Gao et al., Opt. Commun. **93**, 323 (1992); A.S. Zibrov et al., Phys. Rev. Lett. **75**, 1499 (1995)
2. M.O. Scully, Phys. Rev. Lett. **67**, 1855 (1991); M. Fleischhauer et al., Phys. Rev. A **46**, 1468 (1992); A.S. Zibrov et al., Phys. Rev. Lett. **76**, 3935 (1996)
3. M.O. Scully, M. Fleischhauer, Phys. Rev. Lett. **69**, 1360 (1992); A.M. Akulshin, S. Barreiro, A. Lezama, Phys. Rev. A **57**, 2996 (1998); M. Fleischhauer, A.B. Matsko, M.O. Scully, Phys. Rev. A **62**, 013808 (2000); T. Hong, C. Cramer, W. Nagourney, E.N. Fortson, Phys. Rev. Lett. **94**, 050801 (2005)
4. C.H. Bennett, D.P. Divincenzo, Nature **404**, 247 (2000); D. Petrosyan, Y.P. Malakyan, Phys. Rev. A **70**, 023822 (2004); M. Paternostro, M.S. Kim, P.L. Knight, Phys. Rev. A **71**, 022311 (2005)
5. K. Bergmann, H. Theuer, B.W. Shore, Rev. Mod. Phys. **70**, 1003 (1998)
6. S.Y. Zhu, R.C.F. Chan, C.P. Lee, Phys. Rev. A **52**, 710 (1995); S.-Y. Zhu, M.O. Scully, Phys. Rev. Lett. **76**, 388 (1996); P. Zhou, S. Swain, Phys. Rev. Lett. **78**, 832 (1997); P. Zhou, S. Swain, Phys. Rev. A **56**, 3011 (1997); P. Zhou, S. Swain, J. Opt. Soc. Am. B **15**, 2593 (1998); P.R. Berman, Phys. Rev. A **58**, 4886 (1998); K.T. Kapale, M.O. Scully, S.-Y. Zhu, M.S. Zubairy, Phys. Rev. A **67**, 023804 (2003)
7. Ai-Jun Li, Jin-Yue Gao, Jin-Hui Wu, Lei Wang, J. Phys. B. **38**, 3815 (2005)
8. E. Paspalakis, P.L. Knight, Phys. Rev. Lett. **81**, 293 (1998)
9. G.S. Agarwal, *Quantum Optics* (Springer-Verlag, Berlin, 1974)
10. V. Weisskopf, E.P. Wigner, Z. Phys. **54**, 63 (1930)
11. S.-Y. Zhu, R.C.F. Chan, C.P. Lee, Phys. Rev. A **52**, 710 (1994)
12. S.M. Barnett, P.M. Radmore, *Methods in Theoretical Quantum Optics* (Oxford University Press, Oxford, 1997)
13. V. Jyotsna Iyyanki, G.S. Agarwal, Phys. Rev. A **53**, 1690 (1996)
14. H. Lee, P. Poynkin, M.O. Scully, S.-Y. Zhu, Phys. Rev. A **55**, 4454 (1997)